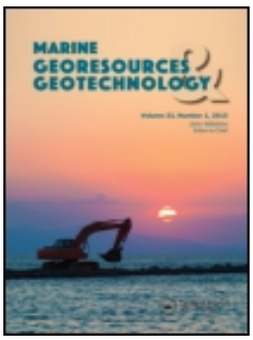

Marine Georesources & Geotechnology

ISSN: 1064-119X (Print) 1521-0618 (Online) Journal homepage: https://www.tandfonline.com/loi/umgt20

Analysis on the effect of salinity in underwater wireless optical communication

Sanjay Kumar, Shanthi Prince, Jinka Venkata Aravind & Santosh Kumar G

To cite this article: Sanjay Kumar, Shanthi Prince, Jinka Venkata Aravind & Santosh Kumar G (2019): Analysis on the effect of salinity in underwater wireless optical communication, Marine Georesources & Geotechnology, DOI: 10.1080/1064119X.2019.1569739

To link to this article: https://doi.org/10.1080/1064119X.2019.1569739

Published online: 14 Feb 2019.

Submit your article to this journal

View Crossmark data

Full Terms & Conditions of access and use can be found at
https://www.tandfonline.com/action/journalInformation?journalCode=umgt20

MARINE GEORESOURCES & GEOTECHNOLOGY
https://doi.org/10.1080/1064119X.2019.1569739

Taylor & Francis
Taylor & Francis Group

Check for updates

Analysis on the effect of salinity in underwater wireless optical communication

Sanjay Kumar, Shanthi Prince, Jinka Venkata Aravind and Santosh Kumar G

Department of ECE, SRM Institute of Science and Technology, SRM Nagar, Kattankulathur, Tamilnadu, India

ABSTRACT

This article deals with the effect of salinity variation on underwater wireless optical communication (UWOC). Effect of different concentration of salt on underwater optical communication has been carried out experimentally in terms of received power at different link lengths. Based on the analysis of experimental data, a mathematical model has been proposed to describe the saline water channel. A simulation study is performed for different data rates and link lengths. It is seen that with increased salinity the attenuation is higher and the UWOC system performance degrades with higher data rate and increased link length.

ARTICLE HISTORY
Received 2 July 2018
Accepted 31 December 2018

KEYWORDS
UWOC; optical turbulence; absorption; scattering; salinity; turbidity

1. Introduction

Underwater wireless information transfer provides a lot of important applications such as oil control, climate change monitoring, pollution monitoring, oceanography research, tactical surveillance, etc. Thus, ocean research and development is of great interest to the military, industry, and scientific community nowadays. In order to employ all the above mentioned applications, a large number of unmanned vehicles or devices are deployed under water. These underwater unmanned vehicles or devices require high data rate and bandwidth for wireless transmission of information (Kaushal and Kaddoum 2016; Zeng et al. 2017; Alomari et al. 2017; Vedachalam et al. 2018).

Current technologies used for wireless communication under water are acoustic wave, radio-frequency wave, and optical wave technologies. Using acoustic wave for transmitting information in underwater wireless communication is the most popular technology because of much lower absorption of acoustic waves in water channel. Thus, it is very useful for long link range communications, ranging up to tens of kilometers. Table 1 provides the performance of acoustic systems under water. Data rates of underwater acoustic communication are limited to tens of kilobits per sec for medium to high range communication. Other limitations of acoustic wave techniques are high latency, high transmission losses, and multipath propagation. In radio-frequency (RF) method, electromagnetic (EM) waves at extremely low frequency (30–300 Hz) are used. For short distances, these EM waves provide high data rate (Kaushal and Kaddoum 2016). Radio frequency waves can undergo a smooth transition through air/water medium but it is highly attenuated in sea water because of salt content being conductive medium. This technique requires bulky and costly transceivers as well as huge transmission antenna (Zeng et al. 2017). As compared to acoustic and RF techniques, underwater wireless optical communication (UWOC) can provide higher transmission bandwidth, higher data rate, better security, low latency, lowest implementation cost, and lower power consumption (Zeng et al. 2017). The comparison of various underwater wireless technologies in terms of different parameters has been tabulated in Table 2. Although, UWOC is advantageous over acoustic and RF techniques in many ways, the main drawback of UWOC is the limited range (less than 100 m) due to different phenomena such as absorption, scattering, and turbulence effects of water channel.

There have been different techniques proposed by various researchers to increase the communication range of UWOC. Multiple-input multiple-output (MIMO) scheme is one of the popular techniques which is widely used to enhance the range of UWOC systems. Jamali and Salehi (2015); Jamali, Salehi, and Akhoundi (2017); Jamali, Nabavi, and Salehi (2018) have extensively studied the performance of MIMO UWOC. Jamali, Salehi and Akhoundi (2017) obtained 8 dB performance improvement in a 25 m coastal water channel by employing a 3 X 1 multiple-input single-output spatial diversity technique. Jamali and Salehi (2015) have proposed mathematical expressions for BER along with its upper bound on the system BER and they have shown that MIMO techniques can enhance the communication range of UWOC systems even in stronger turbulent channel. Zhang and Dong (2016) have proposed a weighted Gamma function polynomial in order to model the impulse response of UWOC MIMO links. This impulse response characterizes the temporal behavior of UWOC channels.

Relay-assisted transmission is another technique employed in UWOC systems in order to enhance the communication range. In order to support longer distances, intermediate relay nodes can be introduced and different

CONTACT Shanthi Prince shanthi.p@ktr.srmuniv.ac.in Department of ECE, SRM Institute of Science and Technology SRM Nagar, Kattankulathur, Tamilnadu 603023, India.

© 2019 Informa UK Limited, trading as Taylor & Francis Group

relaying techniques such as chip detect-and-forward method (Jamali, Akhoundi, and Salehi 2016) decode and forward (DF) relaying (Celik et al. 2018) can be employed for effective communication. Jamali, Akhoundi, and Salehi (2016); Jamali, Chizari, and Salehi (2017) have evaluated the system performance of UWOC in a multi-hop environment. Jamali, Akhoundi, and Salehi (2016) have achieved an improvement of 32 dB in the BER by employing a dual-hop transmission for a communication range of 90 m in a clear ocean channel. Celik et al. (2018) have proposed routing algorithms for relaying techniques such as delay and forward, amplify and forward to enhance the communication range. Jamali, Nabavi, and Salehi (2018) have studied the performance of underwater visible light communication (UVLC) systems. In order to mitigate the fading effects in UVLC systems, the authors have employed MIMO techniques and multiple-symbol detection to overcome the deteriorations due to inter symbol interference.

In order to enhance the performance of UWOC, recently researchers are investigating the factors which limit the performance of UWOC links. Effect of turbulence on UWOC system due to temperature fluctuations in a water channel has been investigated and probability density function of the received optical power is obtained (Vali et al. 2018). Theoretical models have been presented for turbulent water channel and to characterize the channel in terms of absorption and scattering, stochastic model-based equation has been introduced (Zhang et al. 2018). Bai et al. (2018) proposed a time-frequency-domain interleaved orthogonal frequency division multiplexing peak-to-average power ratio reduction scheme for the UWOC system. Under water optical communication system which is fully compatible with 10 Base-T, Ethernet transmission has been designed and demonstrated (Cossu et al. 2018). Mital et al. (2017) reported that characterization of various parameters like luminous flux and bit error rate are important to analyze optical data transmission in different turbid water channels and controlled flow of water. By using polarization division multiplexing and orbital angular momentum multiplexing, an underwater optical link of 12 Gbit/s has been reported (Miller et al. 2017). A modified Rytov method has been used to formulate the scintillation index for a strong turbulent water channel. Channel model is proposed for the heterodyne differential phase shift keying UWOC system considering fading caused by absorption, scattering, and turbulence (Fu and Du 2018). Mattoussi, Khalighi, and Bourennane (2018) demonstrated that performance of UWOC can be enhanced by using channel coding on the upper layers along with the physical layer.

Table 1. Range and bandwidth of acoustic communication system under water for different ranges (Kaushal and Kaddoum 2016).

Distance	Range (km)	Bandwidth (kHz)
Very long	>100	<1
Long	10–100	~ 2-5
Medium	1–10	~10
Short	0.1–1	~10–100
Very short	<0.1	>100

2. Implications of establishing optical link in water

UWOC provides high data rate, larger bandwidth, lower time delay, low latency, low power consumption as compared to acoustic and RF technology but establishing wireless optical link under water is very difficult. The main problem to establish wireless optical link under water is that optical signal is highly affected by optical properties of medium and turbulence induced disturbance (Bosu and Prince 2016).

2.1. Optical properties of water

Absorption and scattering of optical signal are the two main optical properties of water due to which optical signal propagation under water is affected. Absorption and scattering of optical signal depends upon absorption and scattering coefficients. Absorption and scattering coefficients depend on the wavelength of signal and are denoted as $a(\lambda)$ and $b(\lambda)$, respectively. The linear combination of absorption and scattering coefficients is called the beam extinction coefficient $c(\lambda)$ which denotes total attenuation under water and is given as (Kaushal and Kaddoum 2016)

$$c(\lambda) = a(\lambda) + b(\lambda) \quad (1)$$

Depending upon the water type, the value of absorption and scattering coefficients are different, therefore performance of optical wireless link under water depends upon water-clarity. Table 3 (Hanson and Radic 2008) shows that propagation of light is more challenging in turbid harbor as compared to clean ocean.

Mainly four factors are responsible for overall absorption ($a(\lambda)$) and is given by the expression (Jerlov 1976)

Table 3. Absorption and scattering coefficients for different water types (Hanson and Radic 2008).

Water Type	$a(m^{-1})$	$b(m^{-1})$	$c(m^{-1})$
Clear ocean	0.114	0.037	0.151
Coastal ocean	0.179	0.220	0.339
Turbid harbor	0.366	1.829	2.195

Table 2. Comparison of underwater wireless technologies (Kaushal and Kaddoum 2016).

Parameters	Acoustic	RF	Optical
Attenuation	0.1–4 dB/Km	3.5–5dB/Km	0.39 dB/m(ocean) 11 dB/m(turbid)
Latency	High	Moderate	Low
Bandwidth	1–100 KHz (distance dependent)	~ MHz	10–150 MHz
Speed (m/s)	1500	$\sim 2.225 \times 10^8$	$\sim 2.225 \times 10^8$
Range	Up to Kms	Up to ~ 10 m	~ 10–100 m
Data rate	~Kbps	~Mbps	~Gbps
Transmission power	Tens of watts	Few mW to hundreds of watts	Few watts

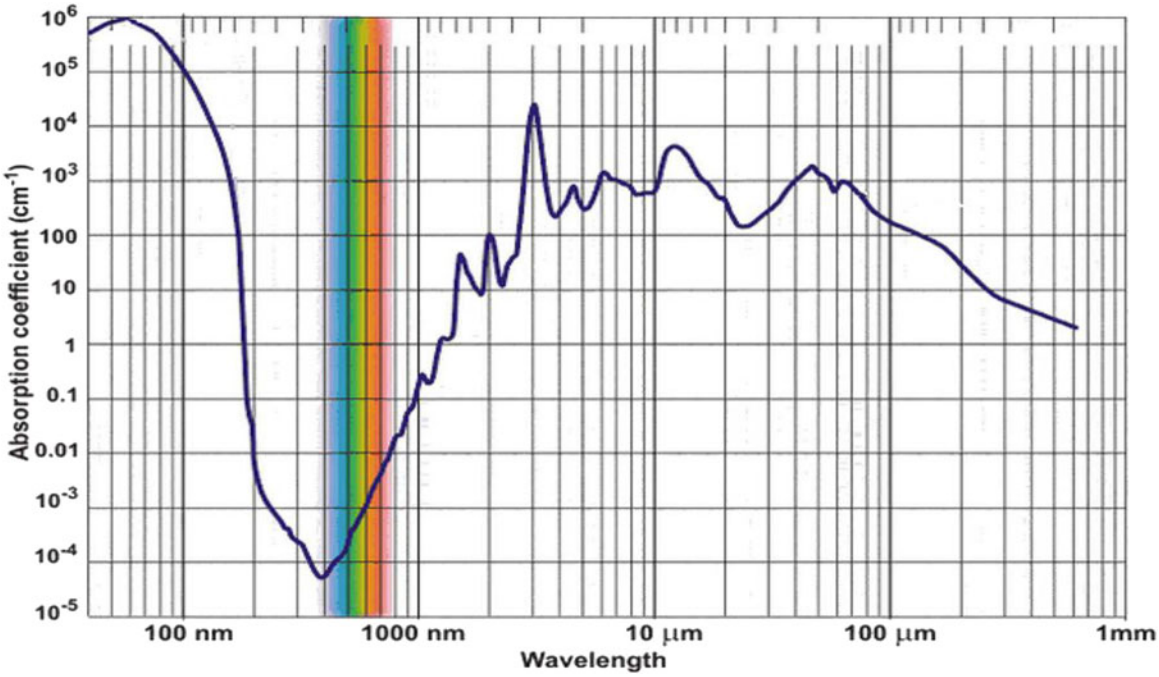

Figure 1. Low attenuation optical window under water (Chaplin 2008).

$$a(\lambda) = C_w a_w(\lambda) + C_{phy} a_{phy}(\lambda) + C_g a_g(\lambda) + C_n a_n\ (\lambda) \quad (2)$$

where $a_w(\lambda)$ denotes the absorption due to pure water, absorption due to phytoplankton is denoted by $a_{phy}\ (\lambda)$, $a_g\ (\lambda)$ denotes the absorption due to Gelbstoff and absorption due to non-algal material suspension is $a_n\ (\lambda)$. C_w, C_{phy}, C_g, and C_n denote the concentration of pure water, phytoplankton, Gelbstoff, and non-algal material, respectively. Light with wavelength from 450 to 550 nm shows a relatively low attenuation property in the sea which corresponds to blue and green spectrum as shown in Figure 1 (Duntley 1963; Chaplin 2008).

Scattering is mainly dependent on the size of suspended particles present in water channel. If the size of the suspended particles is smaller than the wavelength of optical wave used for propagation, the Rayleigh scattering occurs and Mie scattering takes place if the particle size is larger than the wavelength of optical wave. Different regions of ocean water consists of different sizes of suspended particles. In pure ocean water, mostly salts and ions are present whose size is of the order of wavelength of the optical wave used. Therefore, in this case scattering is well described by Rayleigh scattering (Hulburt 1945). Rayleigh scattering coefficient for pure ocean water is given as (Kaushal and Kaddoum 2016)

$$b_w(\lambda) = 0.005826\left(\frac{400}{\lambda}\right)^{4.322} \quad (3)$$

where λ is the wavelength in nm. Scattering plays an important role in shorter wavelength, but overall attenuation in pure ocean water is mainly due to absorption. Ocean water near to land consists of particulate and organic matter. So, attenuation in this case is mainly due to scattering of optical wave. Presence of organic and inorganic particles in ocean water is the main factor for scattering of optical wave. Other factors which are responsible for scattering in sea water are salinity, pressure, temperature which form an optical boundary by changing the refractive index of sea water and deviate the optical wave from its original propagation path. In this case the scattering is well described by Mie scattering. For small and large particles of sea water, the scattering coefficients are given as (Kaushal and Kaddoum 2016)

$$b_l(\lambda) = 1.51302\left(\frac{400}{\lambda}\right)^{1.17} \quad (4)$$

$$b_s(\lambda) = 0.341074\left(\frac{400}{\lambda}\right)^{0.3} \quad (5)$$

where b_l and b_s are scattering coefficients for large and small particles, respectively.

2.2. Turbulence

Apart from absorption and scattering, turbulence is the other main factor that affects the UWOC. Fluctuations in the temperature, density and salinity of the underwater environment lead to variation in the refractive index of underwater channel which results in the fluctuations of the intensity of received signal. This phenomena is called turbulence (Korotkova, Farwell, and Shchepakina 2012; Jamali et al. 2018). Apart from temperature fluctuations and salinity of the underwater environment, air bubbles present in water channel also causes random fluctuations in the refractive index of the water channel (Jamali et al. 2016). Turbulence degrades the performance of UWOC. Therefore effect of turbulence on UWOC has to be analyzed. Mostly experimental investigations have been carried out to study the effect of absorption and scattering on underwater optical

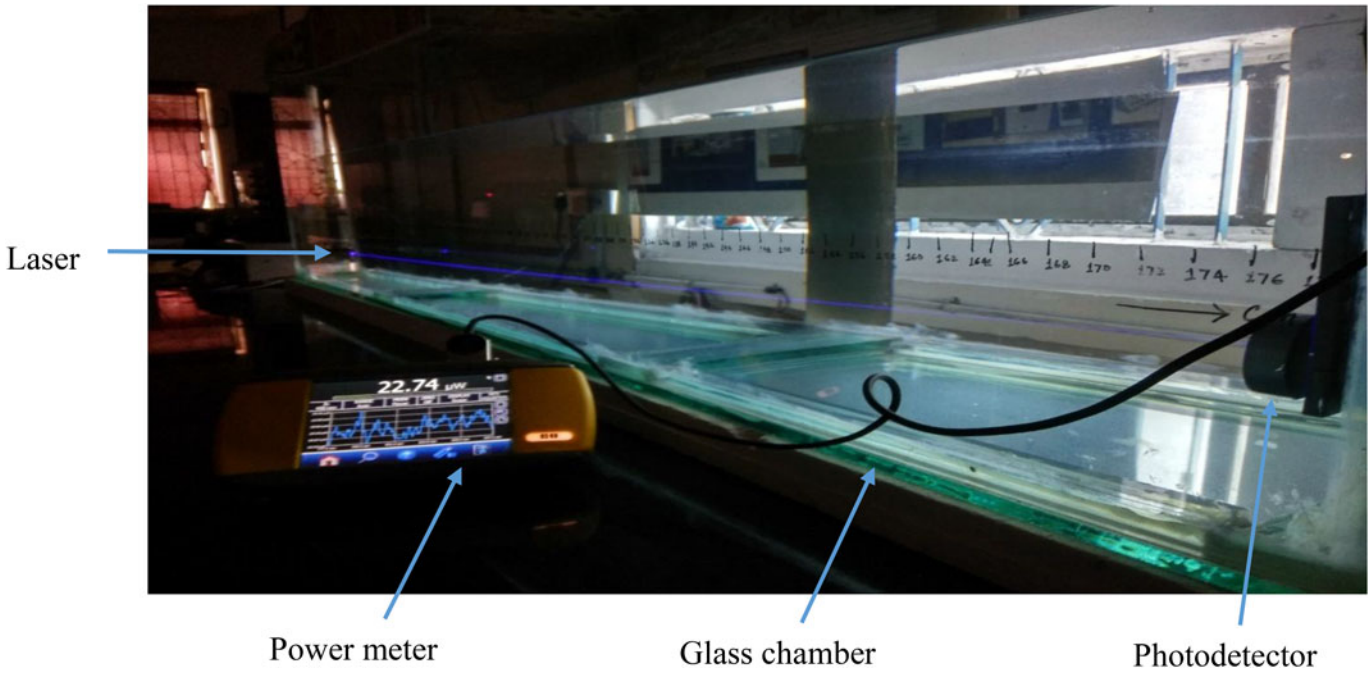

Figure 2. Experimental setup for UWOC.

wireless communication (Kong et al. 2018; Hanson and Radic 2008; Baiden, Bissiri, and Masoti 2009). Komatsu, Markman, and Javidi (2018) proposed a novel signal detection approach for analyzing the effect of background noise. The studies reported have not considered the effect of turbulence on the performance of UWOC system.

In this work, performance of underwater optical wireless communication in terms of received power is experimentally analyzed for water channels with different salinity. A simplified mathematical model for received power as a function of link length and attenuation is proposed based on obtained experimental data. This modeled underwater channel is then imported to OptiSystem with the help of MATLAB. The channel is simulated at different link lengths and performance of UWOC has been studied at different data rates in terms of Q factor and BER.

2.2.1. Salinity in ocean water

Concentration of dissolved salts in water gives the salinity. Salinity is expressed in terms of parts per thousand (ppt) or kilogram of salt in 1000 kilograms of water. Practical salinity unit is given in terms of psu. Salinity in terms of ppt and psu are almost equivalent (Borowski 2009). The average value of salinity in ocean water varies from 31 to 37 ppt. In polar regions, it may be less than 30 ppt. In Antarctic, the salinity range is around 34 ppt. Normally, salinity can be measured by two methods. First one is electrical conductivity (EC) method. EC is measured in terms of micro-siemens/centimeter. Another way to measure salinity is to measure the amount of salt particles present in the solution. This is measured in terms of total dissolved salts. Chlorides, sulfates, sodium carbonate, potassium carbonate, calcium carbonate, and magnesium carbonate are some common salts dissolved in sea water. The typical ocean salinity is around 35 ppt (Boyd 2015) which means that 35 grams of material is dissolved in every 1000 grams of ocean water. As the density of water in CGS unit is 1, 35 grams of material per 1000 gram of water can be expressed as 35 gm/L.

Table 4. Summary of experimental set up parameters.

Components	Parameters	Values
Transmitter	Aperture diameter	20 mm
	Wavelength	450 nm
	Output power	3 mW
	Beam divergence	< 1 mrad
Receiver	Aperture diameter	10 mm
	Spectral range of detection	420–1080 nm
	Noise(peak to peak)	5 pA
	Measurable power	6 nW to 300 mW
Power meter	Power range	4 pW to 30 kW

3. Experimental set-up and observation

In order to study the effect on received optical power as a function of link length for saline water channel, an experimental set-up is established. The experimental set-up comprising of transmitter, receiver, and power meter is shown in Figure 2, and the experimental set-up parameters are summarized in Table 4. Laser diode of wavelength 450 nm and output power of 3 mW is used as transmitter. Signal is transmitted through the saline water channel of known concentration. To emulate the water channel, a glass chamber of dimension 2 m $\times$ 0.45 m $\times$ 0.06 m made of ordinary glass is filled with saline water. The optical signal transmitted through the channel is received by a silicon photodetector and the output power is observed on power meter.

In this experiment, water with different salt concentrations is used as channel and for each channel, received power at different channel length is observed. Minimum average salinity of ocean water is found to be around

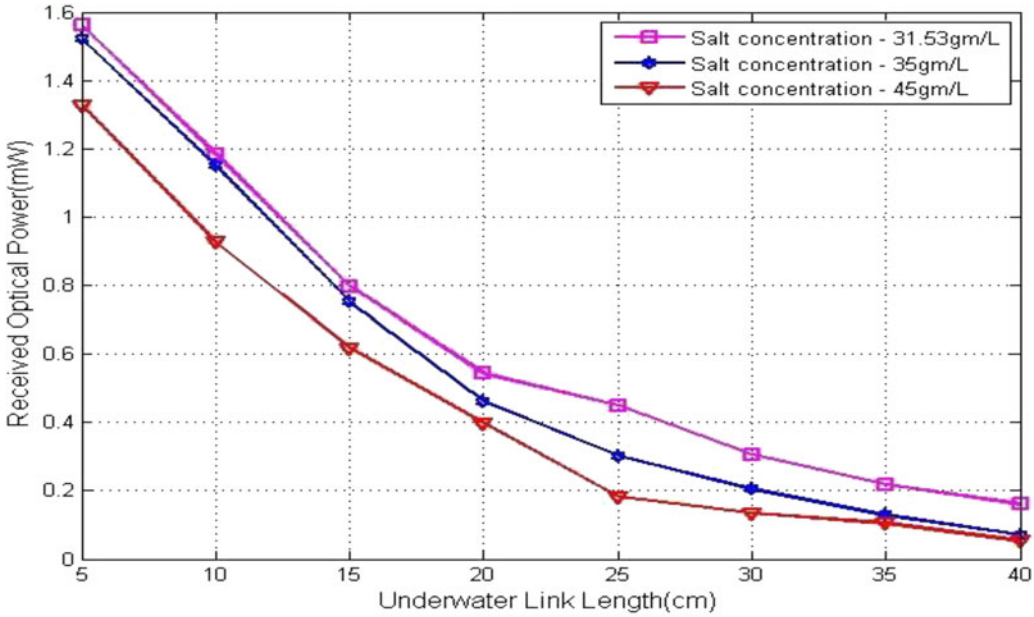

Figure 3. Comparison of received power at different link length for water channel with different salt concentrations.

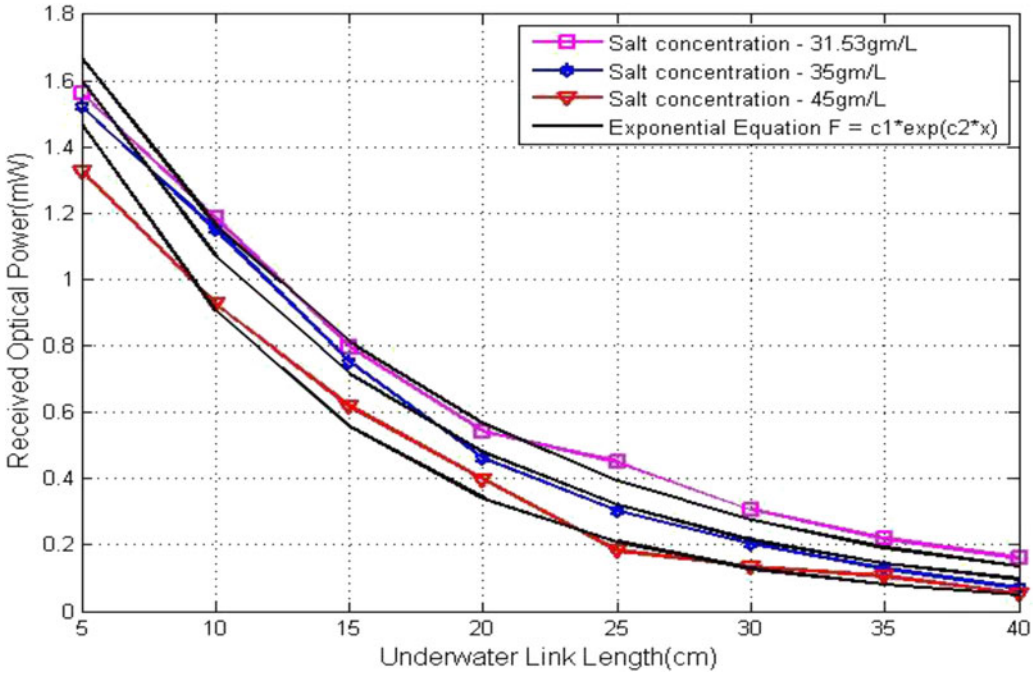

Figure 4. Comparison of analytical and experimental results for water channel with different salt concentrations.

Table 5. Values of constants c_1,c_2 and RMSE values for different salt concentrations.

Salt concentration (gm/L)	c_1	c_2	RMSE values
31.53	2.393	−0.07207	0.0509
35	2.393	−0.08037	0.0471
45	2.393	−0.09731	0.0647

31.5 gm/L, maximum average salinity is found to be 45 gm/L whereas overall average salinity of ocean water is found to be 35 gm/L (Hammer 1986). Thus, salt concentrations of 31.53, 35, and 45 gm/L have been considered while performing the experiment. Figure 3 shows the comparison of received power for different salt concentrations in the water channel.

It is clear from the Figure 3 that in each case received power decreases with link length. It is also observed that received power decreases as salinity increases.

4. Mathematical channel modeling

It is observed from the graphs shown in Figure 3 that there is variation of received power in water channel of different salinity. Therefore, a mathematical expression is needed which can describe the behavior of light propagation in water channel of different salinity. In any medium generally optical signal obeys Beer-Lambert's law (Zeng et al. 2017).

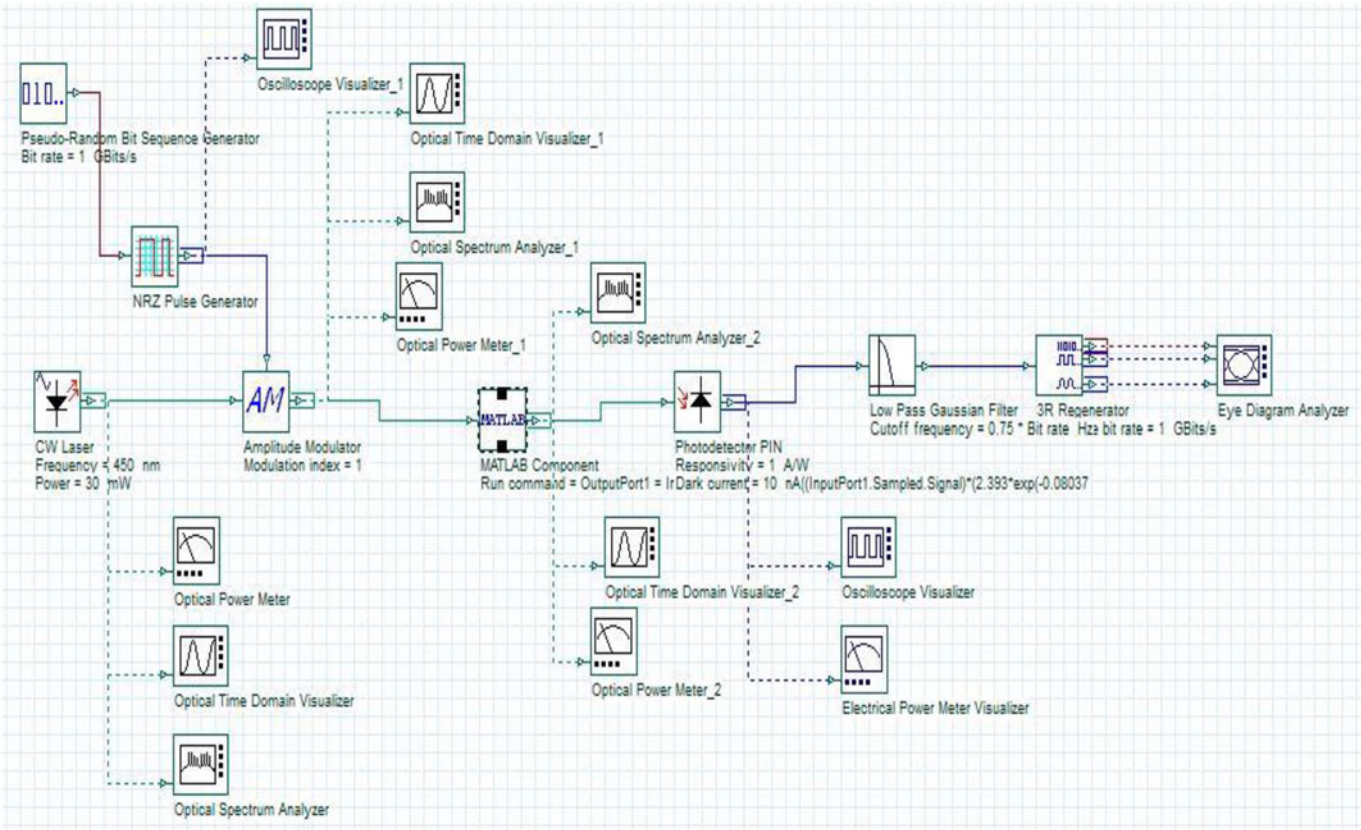

Figure 5. Schematic layout of the proposed UWOC system in OptiSystem.

Table 6. Simulation parameters.

Parameters	Values
Operating wavelength of laser	450 nm
Power of laser	30 mW
Bit rate of bit sequence generator	1 GHz
Amplitude of NRZ pulse	1 a.u.
Modulation index of amplitude modulator	1
Responsivity of photodetector	1 A/W
Dark current of photodetector	10 nA
Cutoff frequency of filter	0.75* Bit rate

Two assumptions have been considered to validate the use of Beer lambert's law in this analysis. First, transmitter and receiver should be perfectly aligned. Second, theoretically, photons which are scattered are lost, however, in real time scenario, some of the scattered photons can be detected by the receiver after multiple scattering (Zeng et al. 2017). As the experiment is performed for a limited range of communication, transmitter and receiver are perfectly aligned. Also, it has been observed during the experiment that the received power level/intensity varies with the link length. As the link length increases, the received power decreases, which suggests that the photons undergo scattering or absorption.

Therefore a simplified mathematical expression is proposed by fitting the obtained experimental data. The mathematical expression is given as

$$p_{r_l} = c_1 * \exp\ (c_2 * \mathrm{x}) \tag{6}$$

where p_{r_l} is the received power at a link length x, c_1, and c_2 are the arbitrary constants. The value of c_1 and c_2 depend upon the salinity and other water properties. The value of c_1 is fixed which takes care of basic attenuation and value of c_2 is fitted based on the salinity. In order to evaluate the constants c_1 and c_2, initially c_1 is estimated and kept constant then for the received power at different salinity, by using curve fitting tool box c_2 is obtained.

Goodness of fit statistics should be examined after using curve fitting to evaluate the accuracy of fit. Root mean square error (RMSE) is one of the parameters which measures the goodness of fit. RMSE value close to zero indicates a good fit. The expression for the RMSE is given as (Chai and Draxler 2014)

$$\mathrm{RMSE} = \sqrt{\frac{\sum_{i=1}^{n} e_i^2}{n}} \tag{7}$$

where "n" is the number of samples of error calculated as e_i(i = 1, 2, 3, … , n).

RMSE value is also obtained from the curve fitting tool.

Figure 4 shows the comparison between analytical and experimental values of received power through water channel with salt concentrations of 31.53, 35, and 45 gm/L. It can be inferred from Figure 4 that analytical and experimental values are almost same. The values of constants c_1, c_2 and RMSE are tabulated in Table 5. It is clear from the Table 5 that root mean square error values are much less which indicates that following Equation (8) best fits for the obtained experimental data.

$$p_{r_l} = 2.393\ \exp\ (-0.08037\mathrm{x});\ \text{for salinity of } 35\mathrm{gm/L} \tag{8}$$

Also, from the Table 5, it can be seen that as the concentration of dissolved salt increases, the constant c_2 also varies.

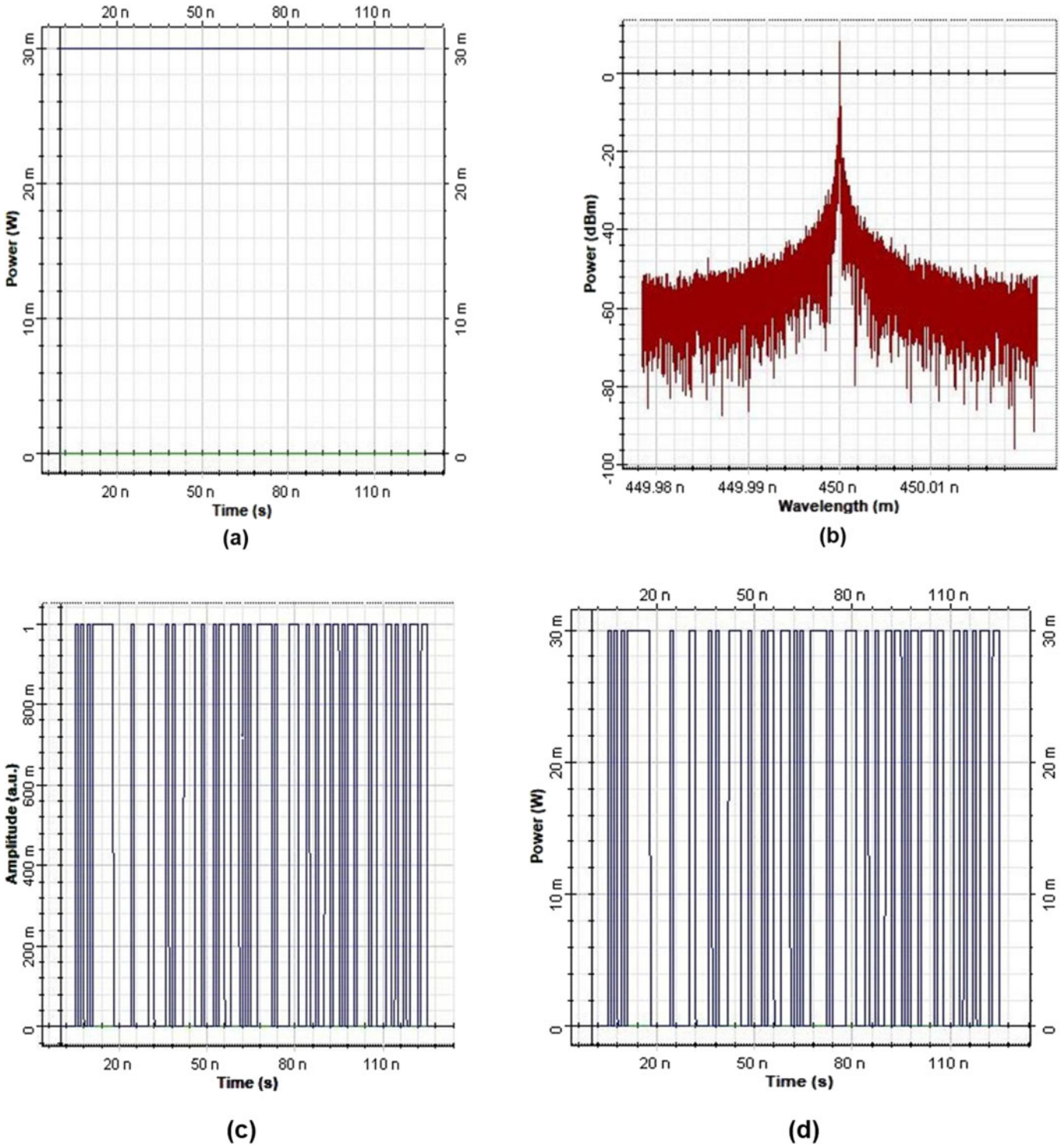

Figure 6. (a) Power of CW laser source. (b) Optical spectrum at the output of laser source. (c) Output of NRZ pulse generator. (d) Output of amplitude modulator (AM). (e) Optical spectrum at the output of AM. (f) Output at the end of underwater channel. (g) Electrical output at photodetector.

5. Performance analysis of UWOC in saline water channel using OptiSystem software

In order to optimize the link length of UWOC system at different data rates, simulation has been carried out by maintaining the acceptable values of BER and Q factor. OptiSystem software is used for simulation. To model the UWOC in saline water channel using Optisystem software, an UWOC channel component is developed by exporting the mathematical equation to the MATLAB component. Mathematical equation is developed by mathematical modeling of the channel using experimental data and MATLAB software. The schematic layout of UWOC in OptiSystem is shown in Figure 5.

Continuous wave laser of wavelength 450 nm and 30 mw is used as transmitter. Outputs of laser and NRZ pulse generator are given to the amplitude modulator of modulation index 1. The output of modulator is given to MATLAB component which is an UWOC channel component developed by using

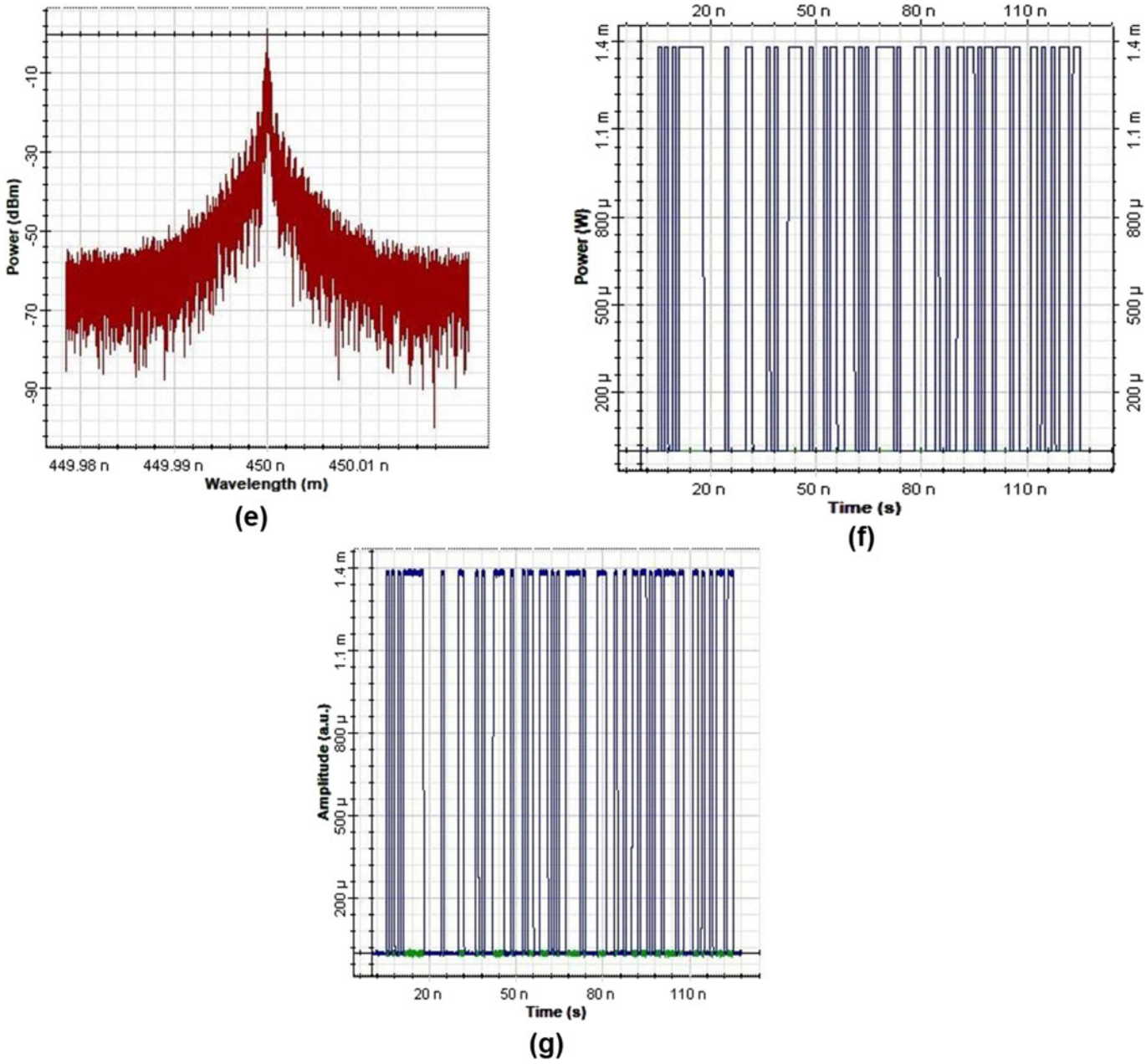

Figure 6. (Continued.)

mathematical equation. PIN photodetector of responsivity 1 A/W and dark current of 10 nA is used as receiver. Low pass filter of cutoff frequency 0.75*Bit rate is used to suppress the noise. 3 R regenerator regenerates original signal from the received signal. Optical power meter, optical time domain visualizer, and optical spectrum analyzer are used to analyze the optical signal whereas oscilloscope visualizer and electrical power meter are used to analyze the electrical signal. To analyze the quality of received signal, eye diagram analyzer is used. Simulation parameters are listed in Table 6.

6. Simulation results

The simulation results of designed UWOC channel in OptiSystem software are presented below. Figure 6a shows the power of the CW laser source whereas Figure 6b represents the optical spectrum of the blue laser source with a peak at wavelength of 450 nm.

Signal generated by the NRZ pulse generator is shown in Figure 6c. It is clear from the Figure 6d that power level of transmission signal is maintained at 30 mW after modulation. It is also clear that operating wavelength is also maintained at 450 nm as depicted in Figure 6e.

Table 7. Performance parameter of simulated UWOC at different link lengths for different data rates.

Data rate	10 Kbps		100 Kbps		1 Gbps	
Link Length (cm)	Q factor	BER	Q factor	BER	Q factor	BER
50	278.318	0	277.835	0	72.396	0
70	268.058	0	208.523	0	3.005	0.001323
100	7.534	2.443×10^{-14}	2.412	0.00791	0	1

Table 8. Performance parameters of received signal.

	Data rate		
Performance parameters	10 Kbps at 101.5 cm	100 Kbps at 94.5 cm	1 Gbps at 66 cm
Q-factor	5.920	5.879	5.738
BER	1.6×10^{-9}	2.058×10^{-9}	4.762×10^{-9}

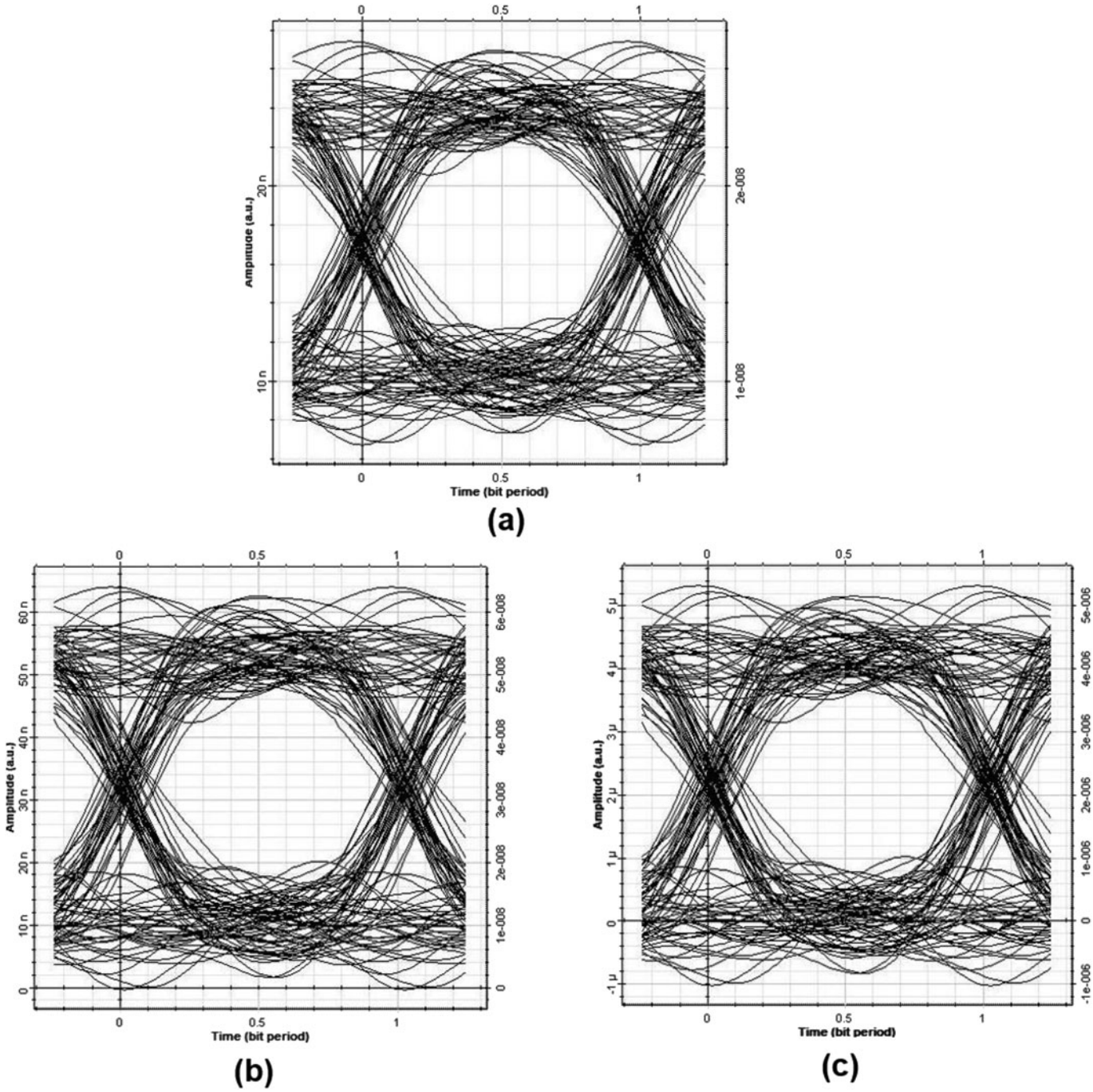

Figure 7. Eye diagram of received signal at (a) 10 Kbps at 101.5cm, (b) 100 Kbps at 94.5cm, and (c) 1 Gbps at 66 cm.

Figure 6f shows the output at the end of underwater channel, the power level of which is considerably attenuated mainly because of absorption and scattering. Electrical output at the photodetector is shown in Figure 6g, the distortion present in the signal is mainly due to ambient noise as well as thermal noise and dark current noise of photodetector.

The simulation has been performed for different underwater link lengths for different data rates. Water channel is modeled at a salt concentration of 35 mg/L which is the average salt concentration present in the ocean. Table 7 shows the performance of the simulated UWOC link in terms of Q factor and BER at different data rates. It can be observed that as the link length increases the performance

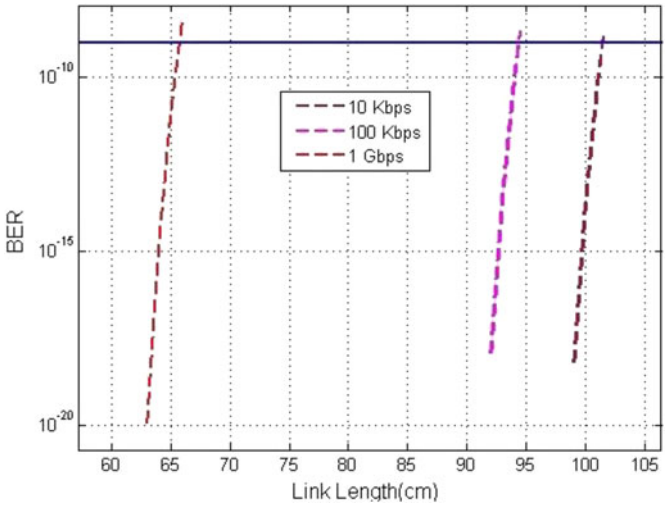

Figure 8. BER vs Link length for different data rates for simulated UWOC.

of the received signal degrades for a given data rate as reflected in the Q factor. Also, UWOC system performance degrades with increased data rate as well. Thus, depending upon the requirement either high data rate system with low link range or low data rate system with high link range can be designed.

For UWOC, the acceptable BER is 10^{-9}. For the simulated data rates, it is found that 1Gbps system performs error free till 66 cm and for lower data rates the admissible range extends which is shown in Table 8. The corresponding eye diagram of the received signal is shown in Figure 7 and BER plot for the simulated UWOC is shown in Figure 8.

From Figure 8, it is seen that with increasing data rates the performance degrades and it limits the admissible link length.

7. Conclusion

Effect of salinity on the performance of UWOC is carried out experimentally. It is found that the received power decreases with increase in concentration of salt in water channel. It is also found that received power also decreases with link length. A mathematical model has been proposed to describe the received power as a function of link length for different concentration of salt in water channel. In order to analyze the performance parameters of received signal of UWOC saline water channel, simulation has been carried out using OptiSystem software and performance parameters are analyzed in terms of Q-factor and BER. Eye diagram is also analyzed which gives the information regarding quality of the received signal. It has been found that Q-factor and BER decrease with link length and quality of signal degrades with increased salinity and data rate.

Acknowledgements

The authors are thankful to SRM - IST for providing infrastructural support.

Disclosure statement

No potential conflict of interest was reported by the authors.

Funding

The authors would like to acknowledge Naval Research Board (NRB) – DRDO, Government of India, for funding this research work under the project reference number NRB/4003/PG/378.

References

Alomari, M. M., M. Wafa, A. Rehab, G. G. Babhair, and M. Hemalatha. 2017. Vision and Challenges of Underwater Optical Wireless Communication-A Survey. *International Journal of Computer Applications* 167 (8): 8–10. doi:10.5120/ijca2017914326.

Baiden, G., Y. Bissiri, and A. Masoti. 2009. Paving the Way for a Future Underwater Omni-Directional Wireless Optical Communication Systems. *Ocean Engineering* 36 (9-10): 633–40. doi:10.1016/j.oceaneng.2009.03.007.

Bai, J., C. Cao, Y. Yang, F. Zhao, X. Xin, A. H. Soliman, and J. Gong. 2018. Peak-to-Average Power Ratio Reduction for DCO-OFDM Underwater Optical Wireless Communication System Based on an Interleaving Technique. *Optical Engineering* 57 (8): 086110. doi:10.1117/1.OE.57.8.086110.

Borowski, B. 2009. Characterization of a very shallow water acoustic communication channel. Paper presented at the MTS/IEEE OCEANS, Biloxi, Mississippi, October 26–29.

Bosu, R., and S. Prince. 2016. Perturbation Methods to Track Wireless Optical Wave Propagation in a Random Medium. *Journal of the Optical Society of America A* 33 (2): 244–50. doi:10.1364/JOSAA.33.000244.

Boyd, C. E. 2015. *Water Quality: An Introduction*. Berlin, Germany: Springer.

Celik, A., N. Saeed, T. Y. Al-Naffouri, and M. S. Alouini. 2018. *Modeling and performance analysis of multihop underwater optical wireless sensor networks. Paper presented at IEEE wireless communications and networking conference (WCNC)*, Barcelona, Spain, April 15–18.

Chai, T., and R. R. Draxler. 2014. Root Mean Square Error (RMSE) or Mean Absolute Error (MAE)?-Arguments Against Avoiding RMSE in the Literature. *Geoscientific Model Development* 7 (3): 1247–50. doi:10.5194/gmd-7-1247-2014.

Chaplin, M. 2008. *Water Absorption Spectrum* 2008-10-24. http://www1.lsbu.ac.uk/water/water_vibrational_spectrum.html

Cossu, G., A. Sturniolo, A. Messa, D. Scaradozzi, and E. Ciaramella. 2018. Full-Fledged 10Base-T Ethernet Underwater Optical Wireless Communication System. *IEEE Journal on Selected Areas in Communications* 36 (1): 194–202. doi:10.1109/JSAC.2017.2774702.

Duntley, S. Q. 1963. Light in the Sea. *Journal of the Optical Society of America* 53 (2): 214–33. doi:10.1364/JOSA.53.000214.

Fu, Y., and Y. Du. 2018. Performance of Heterodyne Differential Phase-Shift-Keying Underwater Wireless Optical Communication Systems in Gamma-Gamma-Distributed Turbulence. *Applied Optics* 57 (9): 2057–63. doi:10.1364/AO.57.002057.

Hammer, U. T. 1986. *Saline Lake Ecosystems of the World*. Vol. 59. Boston, MA: W. Junk Publishers.

Hanson, F., and S. Radic. 2008. High Bandwidth Underwater Optical Communication. *Applied Optics* 47 (2): 277–83. doi:10.1364/AO.47.000277.

Hulburt, E. O. 1945. Optics of Distilled and Natural Water. *Journal of the Optical Society of America* 35 (11): 698–705.

Jamali, M. V., F. Akhoundi, and J. A. Salehi. 2016. Performance Characterization of Relay-Assisted Wireless Optical CDMA Networks in Turbulent Underwater Channel. *IEEE Transactions on Wireless Communications* 15 (6): 4104–16. doi:10.1109/TWC.2016.2533616.

Jamali, M. V., A. Chizari, and J. A. Salehi. 2017. Performance Analysis of Multi-Hop Underwater Wireless Optical Communication Systems. *IEEE Photonics Technology Letters* 29 (5): 462–5. doi:10.1109/LPT.2017.2657228.

Jamali, M. V., P. Khorramshahi, A. Tashakori, A. Chizari, S. Shahsavari, S. Abdollah Ramezani, and J. A. Salehi. 2016. Statistical Distribution of Intensity Fluctuations for Underwater Wireless Optical Channels in the Presence of Air Bubbles. Paper *presented in IEEE Workshop on Communication and Information Theory (IWCIT)*, Yazd, Iran. doi:10.1109/iwcit.2016.7491626.

Jamali, M. V., A. Mirani, A. Parsay, B. Abolhassani, P. Nabavi, A. Chizari, and J. A. Salehi. 2018. Statistical Studies of Fading in Underwater Wireless Optical Channels in the Presence of Air Bubble. *Temperature, and Salinity Random Variations IEEE Transactions on Communications* 66 (10): 4706–23. doi:10.1109/tcomm.2018.2842212.

Jamali, M. V., P. Nabavi, and J. A. Salehi. 2018. MIMO Underwater Visible Light Communications: Comprehensive Channel Study, Performance Analysis, and Multiple-Symbol Detection. *IEEE Transactions on Vehicular Technology* 67 (9): 8223–37. doi:10.1109/TVT.2018.2840505.

Jamali, M. V., and J. A. Salehi. 2015. On the BER of multiple-input multiple-output underwater wireless optical communication systems. Paper p*resented in IEEE 4th International Workshop on Optical Wireless Communications (IWOW)* Istanbul, Turkey. doi:10.1109/iwow.2015.7342259.

Jamali, M. V., J. A. Salehi, and F. Akhoundi. 2017. Performance Studies of Underwater Wireless Optical Communication Systems with Spatial Diversity: MIMO Scheme. *IEEE Transactions on Communications* 65 (3): 1176–92. doi:10.1109/TCOMM.2016.2642943.

Jerlov, N. G. 1976. *Marine Optics*. Vol. 14 of Elsevier Oceanography Series. 2nd ed. Amsterdam: Elsevier.

Kaushal, H., and G. Kaddoum. 2016. Underwater Optical Wireless Communication. *IEEE Access* 4: 1518–47. doi:10.1109/ACCESS.2016.2552538.

Komatsu, S., A. Markman, and B. Javidi. 2018. Optical Sensing and Detection in Turbid Water Using Multidimensional Integral Imaging. *Optics Letters* 43 (14): 3261–4. doi:10.1364/OL.43.003261.

Kong, M., Y. Chen, R. Sarwar, B. Sun, Z. Xu, J. Han, J. Chen, H. Qin, and J. Xu. 2018. Underwater Wireless Optical Communication Using an Arrayed Transmitter/Receiver and Optical Superimposition-Based PAM-4 Signal. *Optics Express* 26 (3): 3087–97. doi:10.1364/OE.26.003087.

Korotkova, O., N. Farwell, and E. Shchepakina. 2012. Light Scintillation in Oceanic Turbulence. *Waves in Random and Complex Media* 22 (2): 260–6. doi:10.1080/17455030.2012.656731.

Mattoussi, F., M. A. Khalighi, and S. Bourennane. 2018. Improving the Performance of Underwater Wireless Optical Communication Links by Channel Coding. *Applied Optics* 57 (9): 2115–20. doi:10.136/ao.57002115.

Miller, J. K., K. S. Morgan, W. Li, Y. Li, I. Srimathi, J. Baghdady, and E. G. Johnson. 2017. *Underwater optical communication link using polarization division multiplexing and orbital angular momentum multiplexing. Paper presented at IEEE OCEANS*, Anchorage, Alaska, USA.

Mital, M. E. G., V. C. Olarte, N. B. S. Ong, D. C. F. Ortega, M. T. R. Uy, J. M. B. Rocamora, and R. R. P. Vicerra. 2017. *Characterization of underwater optical data transmission parameters under varying conditions of turbidity and water movement. Paper presented at 5th IEEE International Conference on Information and Communication Technology (ICoIC7)*, Melaka, Malaysia. doi:10.1109/icoict.2017.8074642.

Vali, Z., A. Gholami, Z. Ghassemlooy, M. Omoomi, and D. G. Michelson. 2018. Experimental Study of the Turbulence Effect on Underwater Optical Wireless Communications. *Applied Optics* 57 (28): 8314–9. doi:10.1364/AO.57.008314.

Vedachalam, N., S. Ramesh, P. U. Prasanth, and G. A. Ramadass. 2018. Modeling of Rising Methane Bubbles During Production Leaks from the Gas Hydrate Sites of India. *Marine Georesources & Geotechnology* 36 (8): 966–73. doi:10.1080/1064119X.2017.1405129.

Zeng, Z., S. Fu, H. Zhang, Y. Dong, and J. Cheng. 2017. A Survey of Underwater Optical Wireless Communications. *IEEE Communications Surveys & Tutorials* 19 (1): 204–38. doi:10.1109/COMST.2016.2618841.

Zhang, H., J. Cheng, Z. Wang, and Y. Dong. 2018. *On the Capacity of Buoy-Based MIMO Systems for Underwater Optical Wireless Links with Turbulence. Paper presented at IEEE international conference on communications (ICC)*, Kansas City, USA, May 20–24. doi:10.1109/icc.2018.8422435.

Zhang, H., and Y. Dong. 2016. Impulse Response Modeling for General Underwater Wireless Optical MIMO Links. *IEEE Communications Magazine* 54 (2): 56–61. doi:10.1109/MCOM.2016.7402261.